A Thermal Switch from Thermoresponsive Polymer Aqueous Solutions

Yunwei Ma

Thesis submitted to the faculty of the

Virginia Polytechnic Institute and State University

In partial fulfillment of the requirements for the degree of

Master of Science

In

Mechanical Engineering

Zhiting Tian, co-chair

Scott Huxtable, co-chair

Thomas Diller

November 29, 2018

Blacksburg, VA

Keywords: Thermal conductivity, Phase change, Transient Grating

A Thermal Switch from Thermoresponsive Polymer Aqueous Solutions

Yunwei Ma

(Academic Abstract)

Thermal switch is very important in today's world and it has varies of applications including heat dissipation and engine efficiency improving. The commercial thermal switch based on mechanical design is very slow and the structure is too complicated to make them smaller. To enable fast thermal switch as well as to make thermal switch more compact, I try to use second order phase transition material to enable our thermal switch. Noticing the transition properties of thermoresponsive polymer for drug delivery, its potential in thermal switch can be expected. I used Poly(N-isopropylacrylamide) (PNIPAM) as an example to show the abrupt thermal conductivity change of thermoresponsive polymer solutions below and above their phase transition temperature. A novel technique, transition grating method, is used to measure the thermal conductivity. The ratio of thermal switch up to 1.15 in transparent PNIPAM solutions after the transition is observed. This work will demonstrate the new design of using second order phase transition material to enable fast and efficient thermal switch.

A Thermal Switch from Thermoresponsive Polymer Aqueous Solutions

Yunwei Ma

(General Audience Abstract)

Controllable thermal conductivity (thermal switching) is very important to thermal management area and useful in a wide area of applications. Nowadays, mechanical thermal conductivity controller device suffers from large scale and slow transition speeds. To solve these problems, I tired the phase transition thermoresponsive polymers to create quick thermal switching because the thermal conductivity will change with the phase. Thermoresponsive polymers show sharp phase changes upon small changes in temperature. Such polymers are already widely used in biomedical-like applications, the thermal switch applications are not well-studied. In this work, I tested Poly(N-isopropylacrylamide) (the abbreviation is PNIPAM) as an example to show the quick thermal conductivity changing ability of thermoresponsive polymer when the transition was happened .I used a novel approach, called the TTG, transient thermal grating. It has easy setup and high sensitivity. The thermal conductivity switching ratio as high as 1.15 in transparent PNIPAM solutions after transition is observed. This work will give new opportunities to control thermal switches using the phase change of thermoresponsive material or abrupt other phase change material in general.

Dedication

This thesis is dedicated to my loving parents, Guoxiong Ma and Ziqun Zhu. For their endless love, support and encouragement

Acknowledgments

First of all, I would like to give my thank my academic advisor, Prof. Zhiting Tian, for her consistent instruction and help throughout the research and the thesis writing.

I also want to thank Prof. Scott Huxtable and Prof. Thomas Diller for their serving as my committee member. Their advice and suggestions are very beneficial to my research and manuscript writing. I would like to express my sincere gratefulness to all the guidance and support from my committee members.

I hope to thank my lab mate, Chen Li and Hao Ma, for their great contribution to the built-up of equipment facility and performing of measurement. This equipment can't work well without the help from them. I also would like to thank my college from CMU and other universities, your kind advice helps us to build this fancy thermal measurement platform.

I will also take this opportunity to thank MingYang, Yuan, Dr. Kornhauser and all my beloved friends. You give me courage in the most difficulty days of research and study, and supports me along the writing of this thesis. I can't be in this position without your encouragement and support.

I must thank my family for their love and support to me throughout my life and during my study at Tech. This thesis can't be made without their support, my love to them is beyond my word.

Last but not least, I would thank to all people who helped in my research and make this thesis real.

Contents

Table of Figures

Nomenclature

Character		Name	Unit
A	=	Laser amplitude	W
c	=	Thermal capacitance	$\frac{J}{kg} \cdot K$
E	=	Power of laser beam	W
L	=	grating constant	m
q	=	Wave vector	$\frac{1}{m}$
R	=	Thermal resistance	$\frac{K}{W}$
t	=	Time	t
T	=	Temperature	K
λ	=	Wavelength	m
ρ	=	Density	$\frac{kg}{m^3}$
φ	=	Phase of laser beam	$radius$
ω	=	Beam size	m
k	=	Thermal conductivity	W/mK
α	=	Thermal diffusivity	m^2/s
θ	=	Incident angle	$radius$

Chapter 1: Introduction

1.1 Background

It's very important to use thermal switch in many applications from space technologies to even smart coffee mugs. The concept and basic design of traditional thermal switches was setup around 1960s for use on space mission to moon, which is still very new.[1-8] Generally, most of the thermal switches use mechanical movement which needs complex structure [9] or phase transitions material [3, 10]. Such traditional mechanical thermal switches can't solve the big size of motors and it is hard to fabricate into small scale. To fabricate a simple designed thermal switch is quite challenging, because it requires a significant change in the thermal conductivity of material used. The thermal switch ratio is defined by the ratio of thermal conductivity after transition to thermal conductivity before transition. In recent works [11-12], the thermos switch ratio from 1.5 to 3.2 are already reported. But all of these first-order phase transition design have significant drawbacks, where latent heat costs more energy and time for transition to happen. Here, I will use the second order phase transition material to enable thermal switch.

Thermoresponsive polymer are the polymer that undergoes a sharp phase transition under temperature change[13-22]. The change is mostly reversible and can be seen from the volume difference [23] around transition temperature. The salvation state change is the physical background behind. It has applications in medical delivery, gene modification and other biomedical area, other applications including battery [24] and sensors [25]. The thermal conductivity potential of thermoresponsive polymer, however, is not fully researched yet.

We can divide the thermoresponsive polymers into two main categories: the first one has a low critical solution temperature (LCST) [26], which means that the polymer become insoluble at high temperature and the other one is upper critical solution temperature (UCST) [27], which means the polymer become soluble at high temperature. The balance of entropy are the main reason for this phase transition[28], where the entropy of chain and entropy of monomers need to find a minimum state. At different temperature the free energy of the mixture will find a minimum with different soluble state [28]. As far as I know, the most studied thermoresponsive polymer is Poly(N-isopropylacrylamide) (PNIPAM) [18, 28-35] , because its transition temperature is 32°C which is close to the body temperature and it can be modified by adding gradients [36]. For thermal energy storage [37] and smart structure application [38], a thermal switch with a room temperature transition activation is strongly preferred. A strong volume change is found for PNIPAM [39] and this phenomenon is very typical for phase transition polymers.

1.2 Aim and objectives

This project is the first attempt of PNIPAM solution thermal switch and also the first attempt of using thermoresponsive polymer. I use a novel technique called transition grating technique to measure the thermal conductivity. A sharp thermal conductivity decreasing was found, this decreasing trend is different from the anticipated result published before[40]. This work is the first to try to apply phase –transition polymers to thermos switch applications, it may also give instructions on using high order phase transition to enable easy and fast thermal switch.

1.3 Publication

Thermal Switching of Thermoresponsive Polymer Aqueous Solutions. Chen Li, Yunwei Ma, and Zhiting Tian. ACS Macro Letters 2018 7 (1), 53-58. DOI: 10.1021/acsmacrolett.7b00938

1.4 Contribution

Chen and Yunwei are both co-first authors to this project. Chen is responsible for the mathematical modeling of thermal grating model and Yunwei is responsible for the graph and table plotting. The optical table setup, sample synthesize and measurement were done by both of them. The main text of submitted paper is mainly written by Chen and the supporting information is mainly written by Yunwei.

1.5 Outline

- Chapter 2 gives a comprehensive review of literature and gives the importance of this work
- Chapter 3 gives the principle of TG and also the numerical model to estimate the results.
- Chapter 4 gives the experimental setup and data acquired.
- Chapter 5 gives the explanation to our experimental result
- Chapter 6 gives the conclusion and also the future potential work

1.6 Summary

This chapter described the background and importance of our work, and briefly introduced the main outcome of our results. Also the publication is given and the construction of this paper is introduced here. The following chapters will follow this organization and gives more details of my research.

Chapter 2: Literature Review

2.1 Thermoresponsive Polymers

Thermoresponsive polymers are sometimes called temperature-responsive polymers, this term refers to polymers that undergoes drastic and discontinuous change of physical properties with temperature. In most of cases, the term is used when the polymer is put in a given solvent and belongs to a larger term called stimuli-responsive materials. Thermoresponsive polymers has a miscibility gap for their solvent-solution diagram, depending on whether this miscibility gap is at high or low temperature, the upper or lower critical temperature can be defined respectively.

PNIPAM is a thermoresponsive polymer which was first synthesized in the 1950s, it can be synthesized with free-radical polymerization and can be functionalized for varies applications. The LCST (lower critical solution temperature) is around 32 ° C. Above LCST, it will transfer from a swollen hydrated state to dehydrate state, losing 90 % of its volume. Its LCST is very close to body temperature, thus, intensive research has been done about its application in tissue engineering and drug delivery. However, the potential of such transition in thermal switch is not fully investigated.

2. 2 Thermal switch

As it is mentioned in the introduction, most of the thermal switch is still made of mechanical switch, whose structure is relatively complicate and big comparing with phase-transition thermal switch, and the reliability is usually lower than phase-transition counterpart. For phase-transition thermal switch the problem is the thermal conductivity k needs to have dramatic change before and after phase transition, as ideally we want to totally turn-on and turn-off the thermal transition.

Another consideration of phase transition thermal switch is that first-order phase transition is not preferred as the latent heat will slow down the transition speed. For example, water and ice has different thermal conductivity but melt ice or cool down water needs to overcome the latent heat. That will make the switch slow and energy inefficient.

2.3 Thermal conductivity measurement

For bulk or thin film or other type of materials, many different method to measure thermal conductivity have been proposed and realized[41]. We can use steady-state measurement or transient hot-wire method [42] to bulk sample. Thin film measurement can use 3ω method [43-47] or time-domain thermoreflectance [48-53]. The traditional measurement technique has obvious drawbacks including extra requirement on sample, more heat contact introduced on sample which lead into large uncertainties [41]. Transient thermal grating (TTG) recently get significant as a new method to measure thermal conductivity for thin films[54-59]. It only needs little sample preparation and can give use high sensitivity and very fast measurement. It is designed by putting two pump beams on to the sample, a thermal grating is thus generated with a temperature difference on the grating [54]. The thermal conductivity will affect how fast this grating will disappear which can be detected by our optical detector.

Chapter 3: Principle of TTG

3.1 Principle

As we can find in Figure 1, my TTG setup is based on transmission measurement and I used heterodyne setup to enhance the signal. [60] Our light source has different wavelength 532 (pump) and 514 nm (probe), and both pump and probe are diffracted by the phase mask. The masking spacing is 3.7 μm, which can generate a grating period L = 1.25 μm. The heating effect needs light absorption but PNIPAM solution is too transparent, so I add food dye (blue) to my sample to enhance the light absorption so the thermal grating can be stronger. After several different attempt, I find the most stable dye for our sample without affect the signal. My sample solution is put in a cuvette with 50 um-thick. I use the sample dye concentration for all the measurement to ensure the sample is under similar heating. The sample temperature is controlled by water bath method. The actual sample temperature on measured spot could be different from heat dissipation, so I used infrared camera to measure the surface temperature and combined with an analytical model to estimate laser heating effect, the final sample temperature is then estimated.

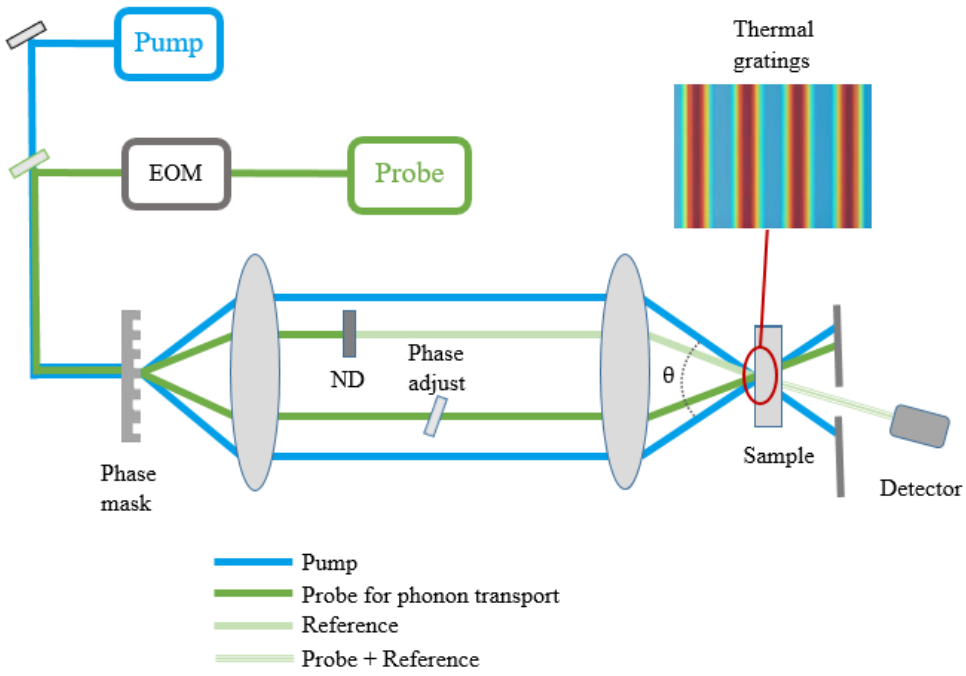

Figure 1. Arrangement of optical path for transient grating method.

3.2 Setup

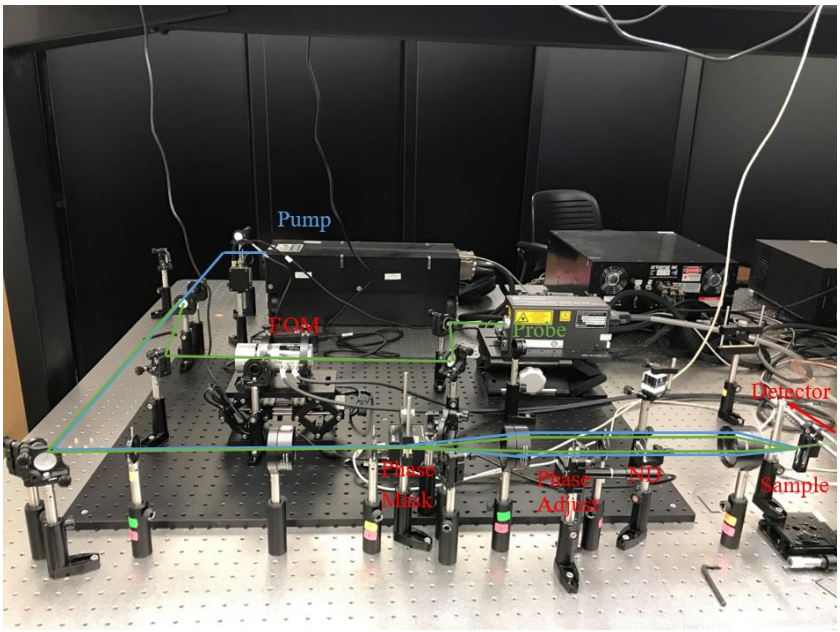

Figure 2. Experimental setup in transmission TTG geometry.

In the TTG setup, a picosecond $Nd:YVO_4$ laser (pulse duration 4-8 ps, wavelength λ_e= 532 nm, frequency 1 kHz, energy 37.5 μJ per pulse) is used for excitation. An electro-optically gated beam from a continuous-wave (CW) solid-state laser (pulse duration 200 μs, wavelength λ_p = 514 nm, CW power 250 mW) is used as the probe beam. The horizontally polarized excitation beam and the vertically polarized probe beam are focused onto the mask with spherical lenses of focal length 15 cm, respectively. To image the mask pattern onto the sample, we use spherical lenses with focal distances f_1 = 15 cm and f_2 = 10 cm. On the sample, the laser spot diameters are about 150 μm for the excitation pulses and about 75 μm for the probe and reference beams. The heterodyne phase is controlled with a motorized actuator by adjusting the angle of a glass plate. The diffracted signal combined with a reference beam, which is derived from the same source and attenuated by a neutral density filter (ND-2), is detected by a balanced amplified photodetector (bandwidth 45 MHz) whose output is recorded with an oscilloscope (4 GHz bandwidth). See the setup in Figure 2.

3.3 Mathematica model

In this part, we use a simple model to explain how the thermal gratings are generated by pump beams and how they dissipate with heat conduction.

A. Formation of thermal gratings

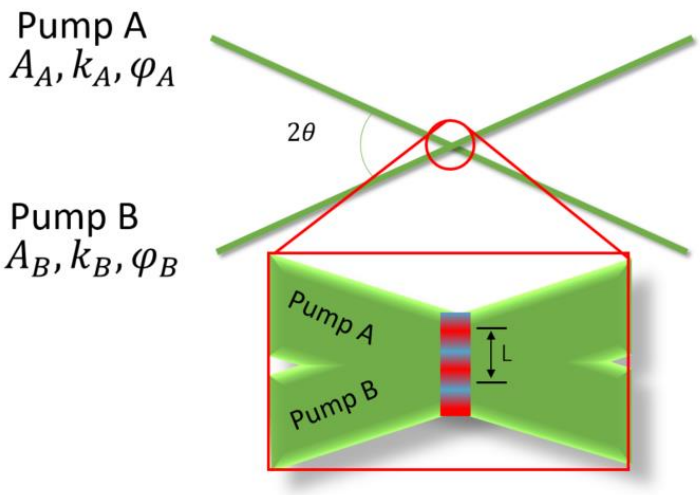

Figure 3. Interference of pump beams.

As shown in Figure 3, two pump beams with amplitude A, wave vector k, phase φ, wavelength $\lambda = 2\pi/k$ are focused on the sample surface and interfere with each other.

The total wave function is expressed as:

$$\mathrm{E} = e^{-i\omega t} \cdot A_A e^{i(\boldsymbol{k_A}\cdot \boldsymbol{r}+\varphi_A)} + e^{-i\omega t} \cdot A_B e^{i(\boldsymbol{k_B}\cdot \boldsymbol{r}+\varphi_B)} \tag{1}$$

Amplitude:

$$|E|^2 = EE^* = {A_A}^2 + {A_B}^2 + 2A_A A_B cos[(\boldsymbol{k_A} - \boldsymbol{k_B}) \cdot \boldsymbol{r} + (\varphi_A - \varphi_B)] \tag{2}$$

In our experiment, $|k_A| = |k_B|$, $|k_A - k_B|$=2k sinθ.

The grating period is:

$$\mathrm{L} = \frac{2\pi}{|k_A - k_B|} = \frac{2\pi}{2\mathrm{k}\ \sin\theta} = \frac{\lambda}{2\ \sin\theta} \tag{3}$$

B. Decay curve of thermal grating

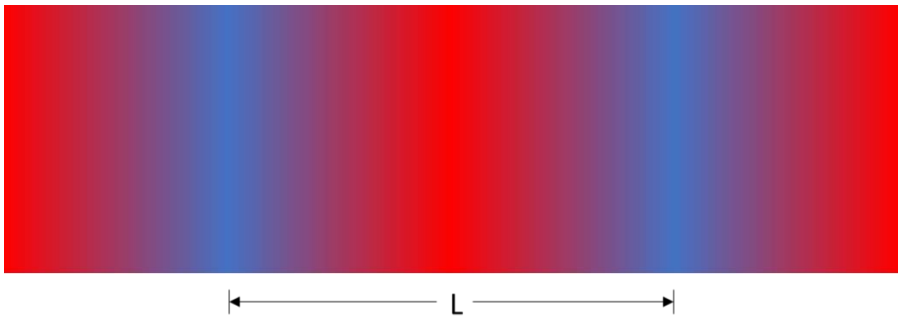

Figure 4. Thermal dissipation of the sample.

Suppose the liquid sample has weak light absorption, the heat is generated uniformly along the beam. Based on the periodic condition, we only consider one grating period with length L and get a one-dimensional heat conduction equation:

$$\rho c \frac{\partial T}{\partial t} = k \frac{\partial^2 T}{\partial x^2} \tag{4}$$

With boundary condition:

$$\frac{\partial T_{(0,t)}}{\partial x} = \frac{\partial T_{(L,t)}}{\partial x} = 0 \tag{5}$$

Initial condition is:

$$T_{(x,0)} = T_\infty + T_0 \cdot \cos\left(2\pi \frac{x}{L}\right) \tag{6}$$

The general solution is:

$$T = T_\infty + T_0 \cdot \sum_{n=1}^{\infty} D_n \cos\left(n\pi \frac{x}{L}\right) e^{\frac{-(n\pi)^2 \cdot \alpha t}{L^2}} \tag{7}$$

Consider initial condition, only n=2 exists. The final solution is

$$T = T_\infty + T_0 \cdot \cos(qx) \cdot e^{-\alpha q^2 t} \tag{8}$$

The above expression shows that temperature decay is an exponential function $e^{-\alpha q^2 t}$. The q can be calculated from optical parameters and the thermal conductivity can be obtained using $k = \rho c_p \alpha$, where ρ is the density and c_p is the specific heat capacity.

3.4 Numerical Model of temperature rise

Along the beam direction, there will be a temperature gradient from water to air. Our IR camera can detect the temperature of outside cuvette, marked as T_{IR}. Here we give a simple estimation of water temperature:

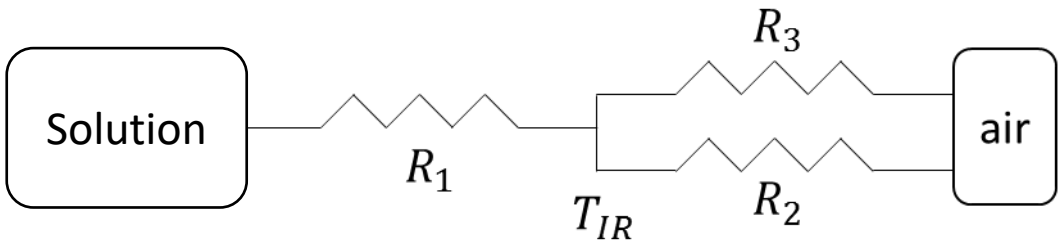

Figure 5. The thermal resistance model for sample. T_{IR} is the temperature detected by IR camera. R_1 is the thermal resistance of water and glass, R_2 is the thermal boundary resistance of cuvette surface and R_3 is the radiation of cuvette surface.

In steady state we have:

$$\dot{q} = \frac{T_{water} - T_{IR}}{R_1} = \frac{T_{IR} - T_{air}}{R_{surface}} \quad (9)$$

And $R_1 = \frac{L_{water}}{k_{water} * A} + \frac{L_{glass}}{k_{glass} * A} = \frac{25 * 10^{-6}\, m}{0.6\, W/mK * 5.625 * 10^{-4} m^2} + \frac{1.25 * 10^{-3}\, m}{1\, W/mK * 5.625 * 10^{-4} m^2} = 2.294\, K/W$ (10)

$$R_{surface} = [R_2^{-1} + R_3^{-1}]^{-1} = \left[\left(\frac{1}{h_{rad} * A}\right)^{-1} + \left(\frac{1}{h_{conv} * A}\right)^{-1}\right]^{-1} = 57.35\, K/W \quad (11)$$

The reference data of thermal conductivity is from [61] and [62]. In this way we calculate sample temperature T_{water} from T_{IR} (°C). Then we made another estimation of laser heating effect and we will prove that it won't impact our sample significantly. Based on steady-state module[63], our average steady state temperature can be described as:

$$\overline{\Delta T} = \frac{\mu * \dot{q}}{k\sqrt{2\pi(\omega_1^2 + \omega_2^2)}} \tag{12}$$

Where $\mu = 0.015$ is laser absorbing ratio, $\dot{q} = 67.5\ mW$ is laser-caused heat flux, k is the thermal conductivity of sample, $\omega_1 = 150\ \mu m$ and $\omega_2 = 75\ \mu m$ are the beam size of pump and probe. The calculated $\overline{\Delta T} \approx 4\ °C$ for all the samples.

Chapter 4: Experimental Result

4.1 PNIPAM solution made

The sample is made by dissolve PNIPAM powder into DI water and do oscillation for 1 h. The dye is added before adding PNIPAM to prevent deposition of PNIPAM. After the oscillation, the sample shows LCST around 32 ° C which confirms its functionality:

a)  (b) 

Figure 6 PNIPAM solution (a) at room temperature and (b) at temperature higher than 32 ℃.

As shown, PNIPAM solution below 32 ℃ is a clear, homogeneous solution while above the 32 ℃ it appears cloudy. We use water bath in the measurements to heat the sample to different temperatures.

4.2 Data acquisition

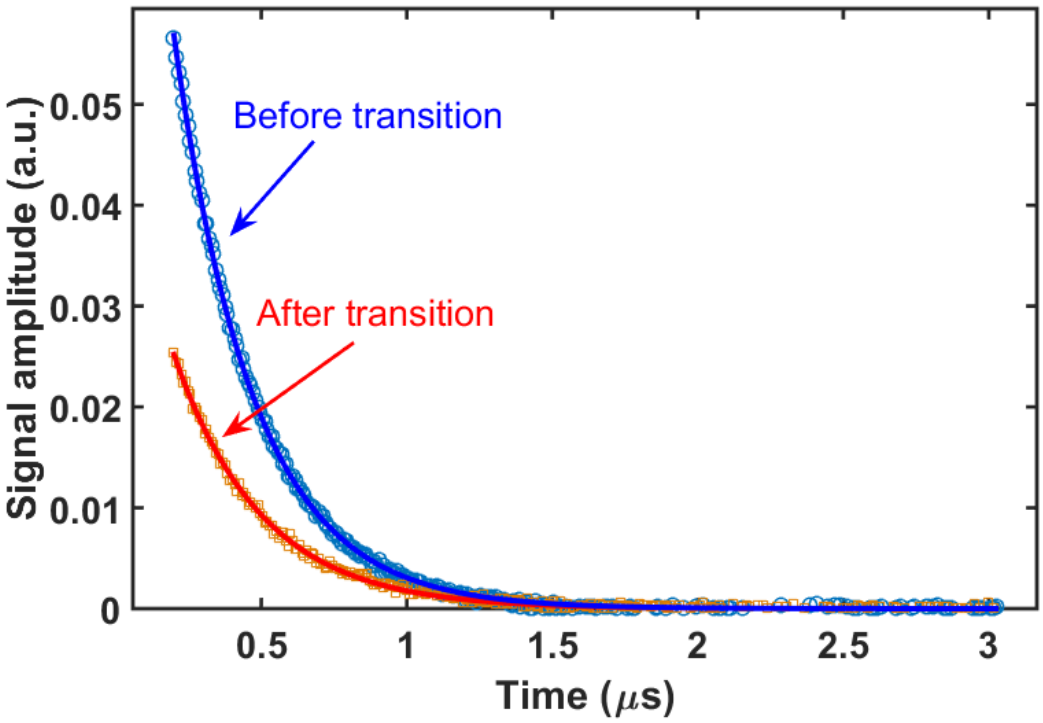

Figure 7 The thermal decay curves of PNIPAM solution across the transition temperature at 0.025 g/ml.

The signal is an exponential decreasing shape, which matches our mathematical model is equation (8). This means that our transient thermal grating model can precisely describe our result here and we can clearly see that after transition the decay curve is more flat, which means the thermal diffusivity is smaller. We assume the thermal capacity and density not changed as most part of the sample solution is water, so we can safely say that the thermal conductivity is also smaller after transition. We did this simplification as thermal conductivity is more straightforward than thermal diffusivity for thermal switch application.

4.3 Experimental Results

To calibrate our TTG measurement setup, I first use water to do the calibration. The measured shows thermal conductivity of 0.611 ± 0.006 W/mK （0.611 is the mean value and 0.006 is the standard deviation） at 25 ℃ and 0.628 ± 0.003 W/mK at 36 ℃, with confidence probability 68.3 %. There is 0.7 % and 0.6 % difference compared with the literature values [64-68] at 25 ℃ and 36 ℃, respectively. Here my standard deviation is also only 1% of mean value. It shows our TTG setup is precise enough. I then moved to measure the PNIPAM sample under different concentration and temperature. The highest concentration is 0.025 g/ml because the sample will become opaque and thus, unable to be measured with our transmission setup. Since the solubility of PNIPAM is higher than 0.025 g/ml, I can safely conclude that the switch ratio can be higher with higher concentration of PNIPAM (the signal intensity drops significantly after transition at 0.025 g/ml as shown in Figure 7).

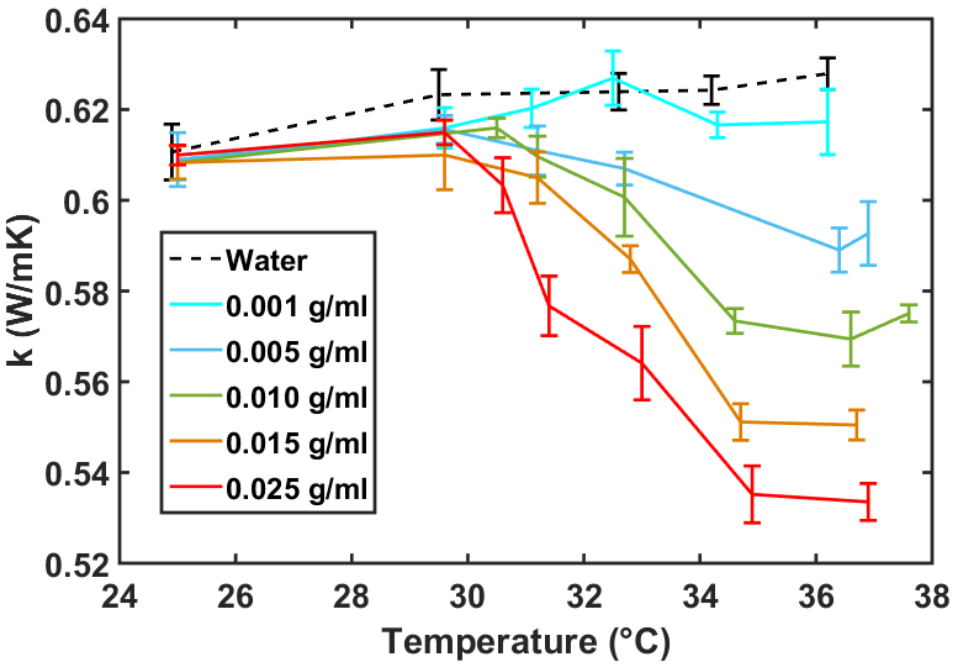

Figure 8 The thermal conductivity of PNIPAM solutions at different concentration and different temperature.

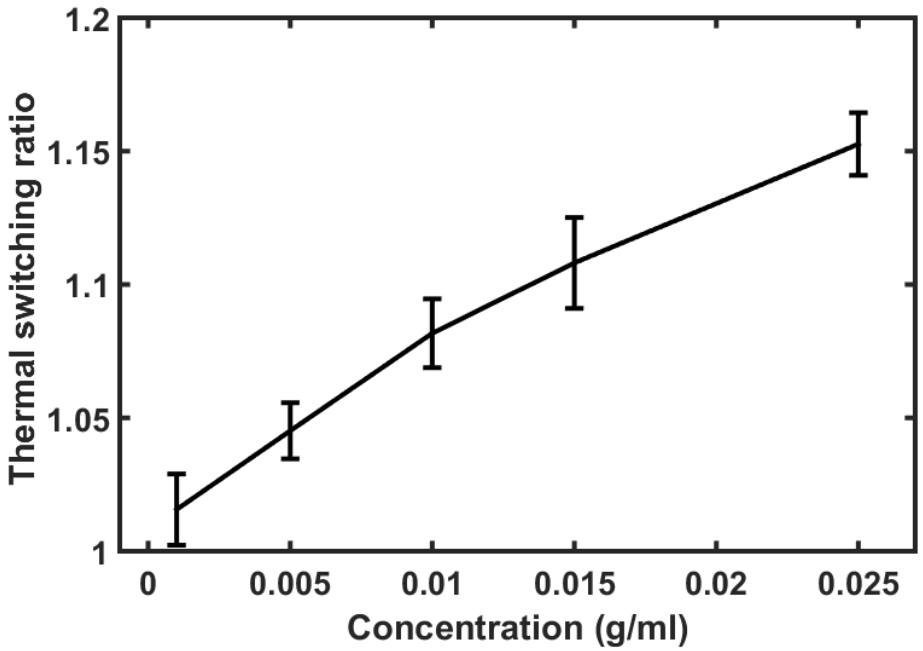

Figure 9 The thermal switching ratio of PNIPAM solution sample at different concentration.

As we can see from Figure 9, the thermal conductivity ratio of PNIPAM is continuously increasing with increased concentration. The highest value I can measure is 1.15 at a concentration of 0.025 g/ml. This data is obtained at a low concentration, so we cannot regard the 15% switching ratio to the only 2.5 % of PNIPAM concentration but only the phase transition. A larger thermal switch ratio can be expected on this plot, however, the transmission requirement limits my experiment to go to high concentration.

Chapter 5: Interpretation and Explanation

5.1 Data interpretation

Before transition, the relatively low thermal conductivity compared with water are found, which supports the lower thermal conductivity for water-polymer sample[69-70]. I also found such mixture has very stable thermal conductivity before transition. When I first heat the sample but not over the transition temperature, the thermal conductivity is first increasing. When the temperature reaches LCST, all sample except the lowest concentration one with 0.001 g/ml, has a sharp thermal conductivity decreasing. The transition time is very fast with milliseconds [71] because it is a second order phase transition without any latent heat to slow down the process.

5.2 Explanation of result

The trend we found is different from the previous report [40] that thermal conductivity of PNIPAM water solution has increased thermal conductivity above the transition temperature LCST. To explain my recording, here is the physical explanation. With strong intermolecular hydrogen bonding with water molecules below LCST, the PNIPAM is soluble. When heated above LCST, the hydrogen bound between PNIPAM chain and water molecules break[31, 72], meanwhile the chain folds with intramolecular hydrogen bonds become dominant[73-74]. As we can see in Figure 10, such change will result in a shrink in volume and will create a water phase and PNIPAM phase. Consider the research claiming that hydrophility has better thermal transport at solid-liquid interfaces compared with hydrophobicity [75-77]. I attribute the lowered thermal conductivity above LCST to the thermal interface resistance between water and shrinked PNIPAM molecules, which were soluble with no interface resistance under LCST[78].

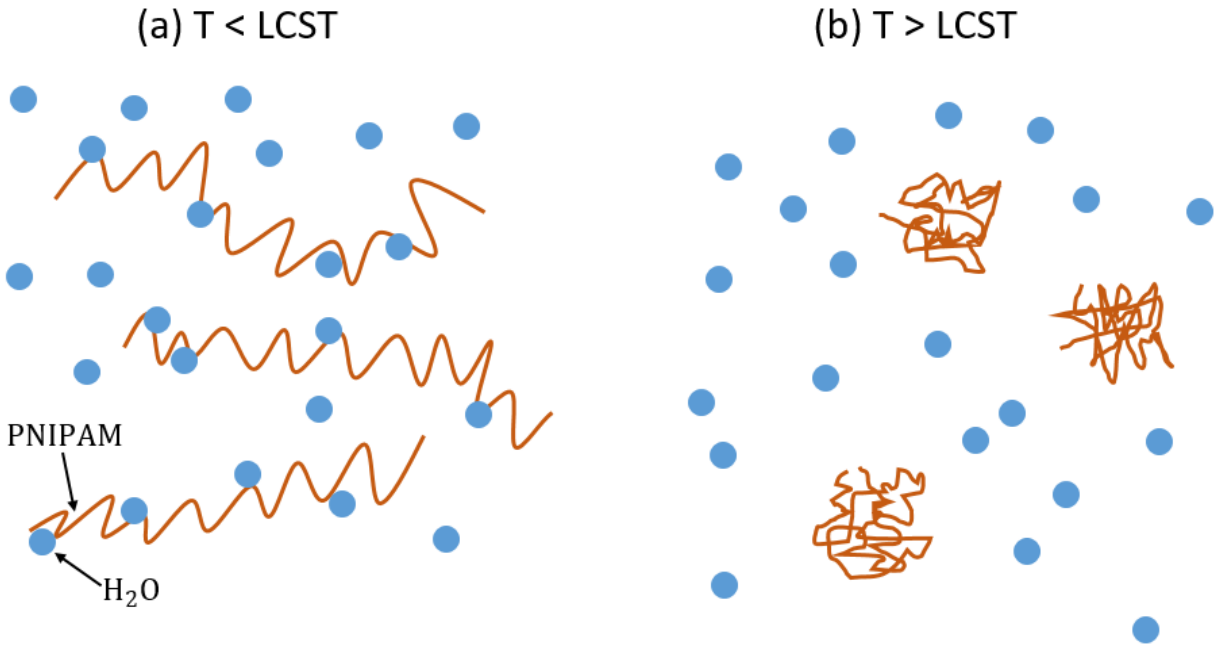

Figure 10 The illustration of PNIPAM solution (a) below and (b) above transition temperature.

Chapter 6: Conclusion and Future Work

6.1 Conclusion

In conclusion, I use a novel measurement technique, the transient thermal grating technique to measure the thermal switch behavior of thermoresponsive polymer PNIPAM. A thermal switching ratio of 1.15 in transparent PNIPAM solution with concentration 0.025 g/ml above LCST was found. The second order phase transition property can enable fast switching and compact design. As far as I know, it is the first time to apply high order phase transition phenomenon into thermal switch. This project will give information on the minimization of thermal switch and the switch frequency optimization.

6.2 Future Work

One of the disadvantage is the switch ratio is only 15% in our experiment which is much lower than transitional mechanical switch. Our TTG is based on transmission laser measurement so we can't measure high concentration which is opaque. So further experiment can be made through non-transmission measurement to test higher PNIPAM concentration.

Another potential research is about PNIPAM hydrogel. PNIPAM hydrogel is already observed to have similar phase-transition property with PNIPAM solution. With higher PNIPAM concentration, its hydrogel may give us higher thermal switch ratio.

Appendix A: Water Bath Temperature Monitor

IR camera is used to monitor the temperature of sample controlled by water bath. It can be see that at 32℃ water bath, our sample temperature is around 28℃. If we add 28℃ with the laser heating effect (4℃, estimated from equation (12)), we get 32℃, the LCST of PNIPAM.

<table>
<tr><td> 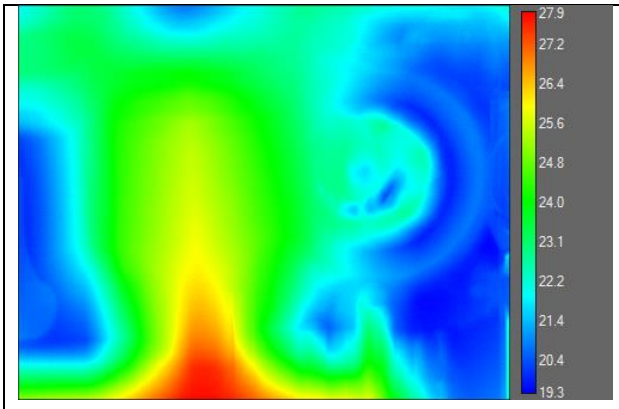
</td><td> 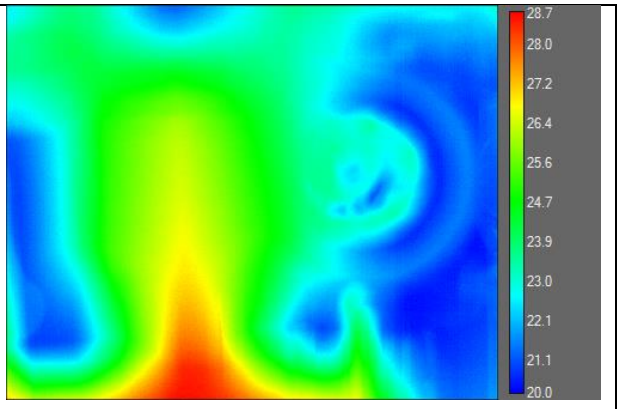
</td></tr>
<tr><td>32℃</td><td>33℃</td></tr>
<tr><td> 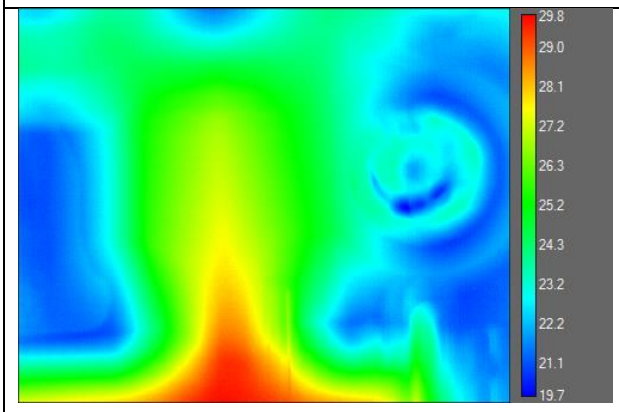
</td><td> 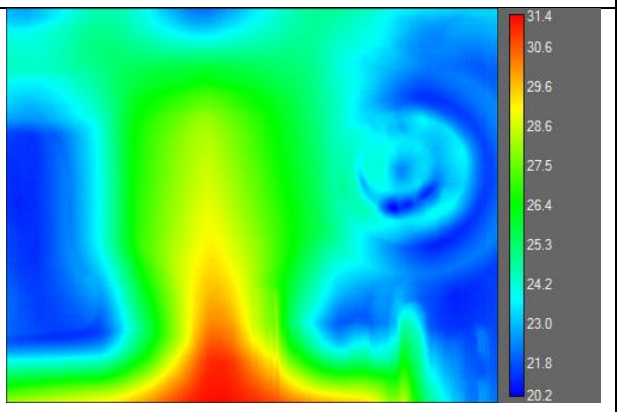
</td></tr>
<tr><td>34℃</td><td>36℃</td></tr>
</table>

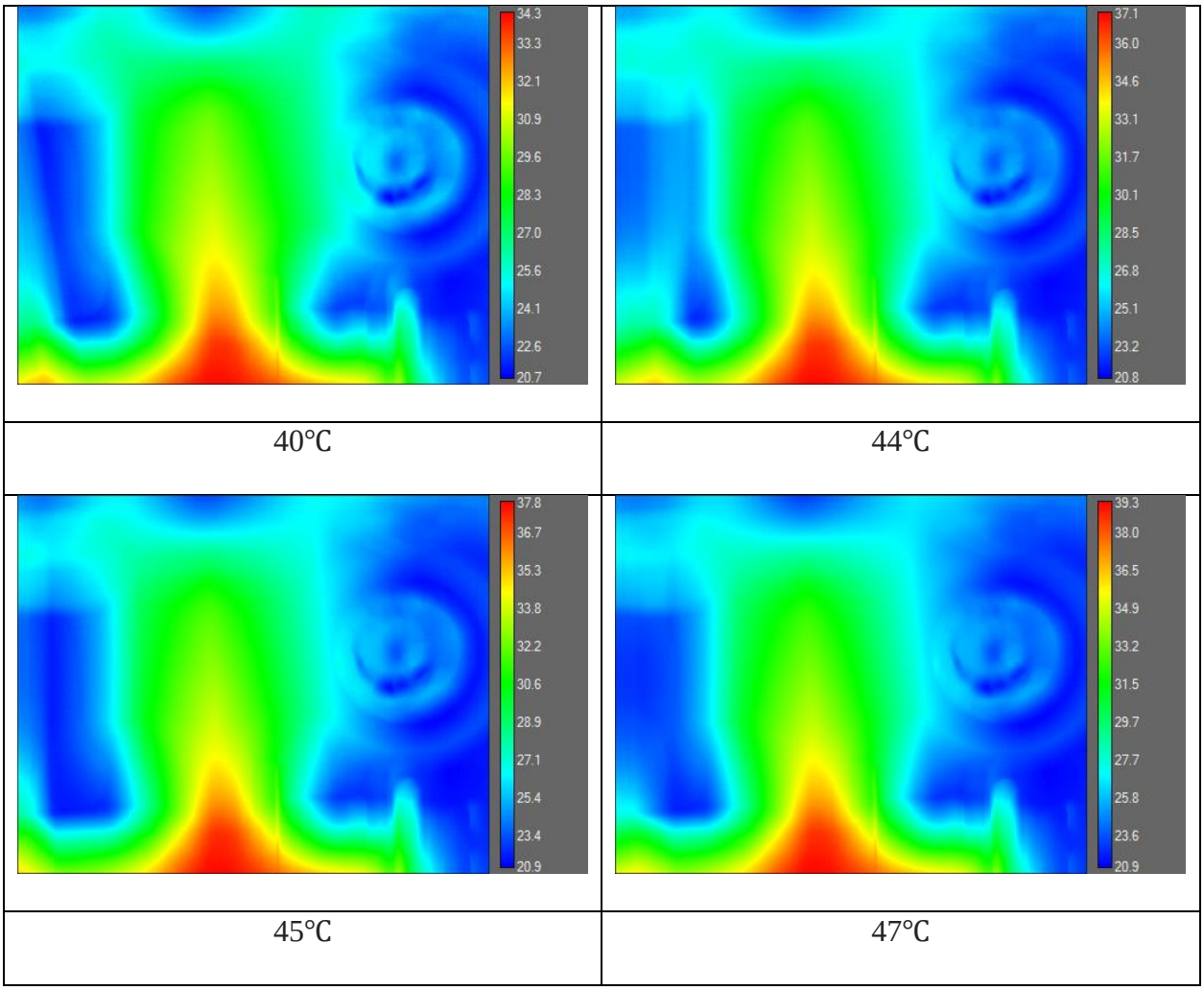

40℃	44℃
45℃	47℃

Figure 11 IR camera result of temperature rising of sample cuvette.

Appendix B: Controlled Experiment of Scattering and Polymer type

We measured $Ca(OH)_2$ aqueous suspensions at different concentrations (0.01 – 0.025 g/mL) to simulate the increased light scattering when the phase transition of PNIPAM aqueous solutions happens, and to test whether it would affect the results.

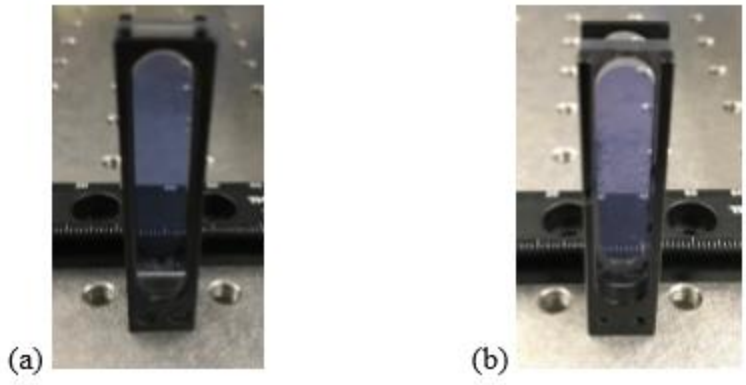

Figure 12 $Ca(OH)_2$ aqueous suspensions of (a) 0.01 g/mL and (b) 0.025 g/mL.

The result is shown in the table below, we can see that the stronger light scattering comes from higher $Ca(OH)_2$ won't led into higher measured k. This proves that the decrease of k in our PNIPAM sample above LCST does not come from light scattering.

Table A1. Thermal conductivities of $Ca(OH)_2$ aqueous suspensions at room temperature

Concentrations (g/mL)	0.01	0.015	0.02	0.025
Thermal conductivity (W/mK)	0.602 ±0.004	0.600 ±0.005	0.607 ±0.002	0.601 ±0.005

As shown in Figure A3, we measured PNIPAM aqueous solutions of 0.015 g/mL with two different polymer molecular weights (Mn). PNIPAM A has an average Mn of 30,000, with Mn between 25,000 and 35,000, and poly-dispersity $\leqslant$1.5 (narrow chain length distribution), while PNIPAM B has Mn ranging from 20,000 to 40,000. We assume that the different polymer molecular weights would affect the light scattering above the LCST. The determined thermal conductivities are close to each other.

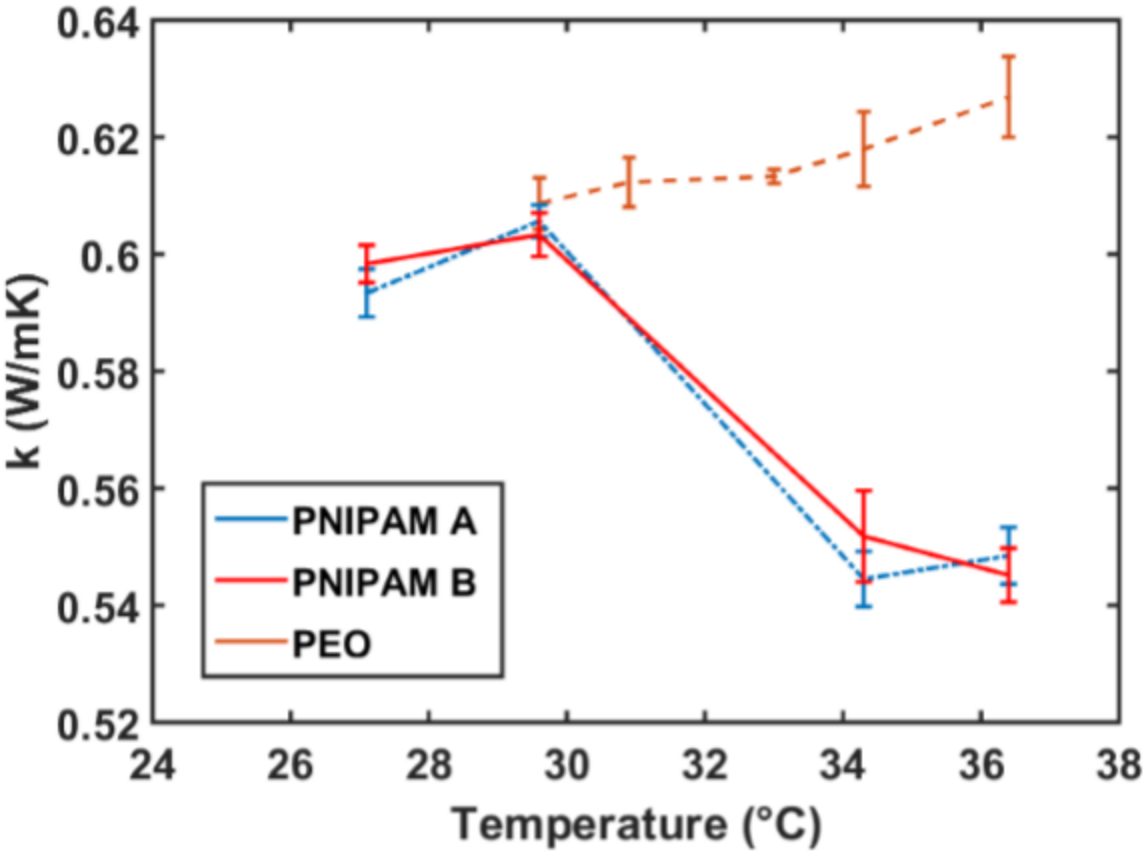

Figure 13 The thermal conductivity change vs. temperature for PNIPAM (different molecular mass) and PEO.

We also conducted another control experiments to show that the drastic thermal conductivity change is not observed in a non-thermoresponsive polymer aqueous solution without an LCST behavior. We chose Poly(ethylene oxide) (PEO) aqueous solution of 0.015 g/mL, and the measured thermal conductivity as a function of temperature simply follows the trend of water.

References

1. Ng, B. T.; Lim, Z. Y.; Hung, Y. M.; Tan, M. K., Phase change modulated thermal switch and enhanced performance enabled by graphene coating. *RSC Advances* **2016,** *6* (90), 87159-87168.
2. Wang, Y.; Schwartz, D. E.; Smullin, S. J.; Wang, Q.; Sheridan, M. J., Silicon Heat Switches for Electrocaloric Cooling. *Journal of Microelectromechanical Systems* **2017,** *26* (3), 580-587.
3. Yang, Y.; Basu, S.; Wang, L., Vacuum thermal switch made of phase transition materials considering thin film and substrate effects. *Journal of Quantitative Spectroscopy and Radiative Transfer* **2015,** *158*, 69-77.
4. Chiou, J.-C.; Chou, L.-C.; Lai, Y.-L.; Huang, S.-C., A novel thermal switch and variable capacitance implement by CMOS MEMS process approaching in micro electrostatic converter. *Solid-State Electronics* **2012,** *77*, 56-63.
5. He, J.-H.; Singamaneni, S.; Ho, C. H.; Lin, Y.-H.; McConney, M. E.; Tsukruk, V. V., A thermal sensor and switch based on a plasma polymer/ZnO suspended nanobelt bimorph structure. *Nanotechnology* **2009,** *20* (6), 065502.
6. McKay, I. S.; Wang, E. N., Thermal pulse energy harvesting. *Energy* **2013,** *57*, 632-640.
7. Cho, J.; Wiser, T.; Richards, C.; Bahr, D.; Richards, R., Fabrication and characterization of a thermal switch. *Sensors and Actuators A: Physical* **2007,** *133* (1), 55-63.
8. Cho, J.; Richards, C.; Bahr, D.; Jiao, J.; Richards, R., Evaluation of contacts for a MEMS thermal switch. *Journal of Micromechanics and Microengineering* **2008,** *18* (10), 105012.
9. DiPirro, M. J.; Shirron, P. J., Heat switches for ADRs. *Cryogenics* **2014,** *62*, 172-176.
10. Kim, K.; Kaviany, M., Thermal conductivity switch: Optimal semiconductor/metal melting transition. *Physical Review B* **2016,** *94* (15), 155203.
11. Warzoha, R. J.; Weigand, R. M.; Fleischer, A. S., Temperature-dependent thermal properties of a paraffin phase change material embedded with herringbone style graphite nanofibers. *Applied Energy* **2015,** *137*, 716-725.
12. Zheng, R.; Gao, J.; Wang, J.; Chen, G., Reversible temperature regulation of electrical and thermal conductivity using liquid–solid phase transitions. *Nature communications* **2011,** *2*, 289.
13. Wei, M.; Gao, Y.; Li, X.; Serpe, M. J., Stimuli-responsive polymers and their applications. *Polymer Chemistry* **2017,** *8* (1), 127-143.
14. Hoffman, A. S. In *"Intelligent" polymers in medicine and biotechnology*, Macromolecular symposia, Wiley Online Library: 1995; pp 645-664.
15. Galaev, I.; Mattiasson, B., *Smart polymers: applications in biotechnology and biomedicine*. CRC Press: 2007.
16. Theato, P., Synthesis of well‐defined polymeric activated esters. *Journal of Polymer Science Part A: Polymer Chemistry* **2008,** *46* (20), 6677-6687.
17. Dai, S.; Ravi, P.; Tam, K. C., pH-Responsive polymers: synthesis, properties and applications. *Soft Matter* **2008,** *4* (3), 435-449.
18. Heskins, M.; Guillet, J. E., Solution properties of poly (N-isopropylacrylamide). *Journal of Macromolecular Science—Chemistry* **1968,** *2* (8), 1441-1455.
19. Davis, D. A.; Hamilton, A.; Yang, J.; Cremar, L. D.; Van Gough, D.; Potisek, S. L.; Ong, M. T.; Braun, P. V.; Martínez, T. J.; White, S. R., Force-induced activation of covalent bonds in mechanoresponsive polymeric materials. *Nature* **2009,** *459* (7243), 68.
20. Colson, Y. L.; Grinstaff, M. W., Biologically responsive polymeric nanoparticles for drug delivery. *Advanced Materials* **2012,** *24* (28), 3878-3886.
21. Piskin, E., Stimuli-responsive polymers in gene delivery. *Expert review of medical devices* **2005,** *2* (4), 501-509.
22. Stuart, M. A. C.; Huck, W. T.; Genzer, J.; Müller, M.; Ober, C.; Stamm, M.; Sukhorukov, G. B.; Szleifer, I.; Tsukruk, V. V.; Urban, M., Emerging applications of stimuli-responsive polymer materials. *Nature materials* **2010,** *9* (2), 101.
23. Kim, Y.-J.; Matsunaga, Y. T., Thermo-responsive polymers and their application as smart biomaterials. *Journal of Materials Chemistry B* **2017**.
24. Chen, Z.; Hsu, P.-C.; Lopez, J.; Li, Y.; To, J. W.; Liu, N.; Wang, C.; Andrews, S. C.; Liu, J.; Cui, Y., Fast and reversible thermoresponsive polymer switching materials for safer batteries. *Nature Energy* **2016,** *1*, 15009.
25. Hu, J.; Liu, S., Responsive polymers for detection and sensing applications: current status and future developments. *Macromolecules* **2010,** *43* (20), 8315-8330.

26. Charlet, G.; Delmas, G., Thermodynamic properties of polyolefin solutions at high temperature: 1. Lower critical solubility temperatures of polyethylene, polypropylene and ethylene-propylene copolymers in hydrocarbon solvents. *Polymer* **1981,** *22* (9), 1181-1189.
27. Baker, C.; Brown, W.; Gee, G.; Rowlinson, J.; Stubley, D.; Yeadon, R., A study of the thermodynamic properties and phase equilibria of solutions of polyisobutene in n-pentane. *Polymer* **1962,** *3*, 215-230.
28. Geryak, R.; Tsukruk, V. V., Reconfigurable and actuating structures from soft materials. *Soft matter* **2014,** *10* (9), 1246-1263.
29. Feil, H.; Bae, Y. H.; Feijen, J.; Kim, S. W., Effect of comonomer hydrophilicity and ionization on the lower critical solution temperature of N-isopropylacrylamide copolymers. *Macromolecules* **1993,** *26* (10), 2496-2500.
30. Okada, Y.; Tanaka, F., Cooperative hydration, chain collapse, and flat LCST behavior in aqueous poly (N-isopropylacrylamide) solutions. *Macromolecules* **2005,** *38* (10), 4465-4471.
31. Schild, H. G., Poly (N-isopropylacrylamide): experiment, theory and application. *Progress in polymer science* **1992,** *17* (2), 163-249.
32. Dong, X.; Chen, S.; Zhou, J.; Wang, L.; Zha, L., Self-assembly of monodisperse composite microgels with bimetallic nanorods as core and PNIPAM as shell into close-packed monolayers and SERS efficiency. *Materials & Design* **2016,** *104*, 303-311.
33. Feng, X.; Zhang, K.; Chen, P.; Sui, X.; Hempenius, M. A.; Liedberg, B.; Vancso, G. J., Highly Swellable, Dual‐Responsive Hydrogels Based on PNIPAM and Redox Active Poly (ferrocenylsilane) Poly (ionic liquid) s: Synthesis, Structure, and Properties. *Macromolecular rapid communications* **2016,** *37* (23), 1939-1944.
34. Pelton, R., Poly (N-isopropylacrylamide)(PNIPAM) is never hydrophobic. *Journal of colloid and interface science* **2010,** *348* (2), 673-674.
35. Shi, Y.; Ma, C.; Peng, L.; Yu, G., Conductive "Smart" Hybrid Hydrogels with PNIPAM and Nanostructured Conductive Polymers. *Advanced Functional Materials* **2015,** *25* (8), 1219-1225.
36. James, H. P.; John, R.; Alex, A.; Anoop, K., Smart polymers for the controlled delivery of drugs–a concise overview. *Acta Pharmaceutica Sinica B* **2014,** *4* (2), 120-127.
37. Regin, A. F.; Solanki, S.; Saini, J., Heat transfer characteristics of thermal energy storage system using PCM capsules: a review. *Renewable and Sustainable Energy Reviews* **2008,** *12* (9), 2438-2458.
38. Khudhair, A. M.; Farid, M. M., A review on energy conservation in building applications with thermal storage by latent heat using phase change materials. *Energy conversion and management* **2004,** *45* (2), 263-275.
39. HAMANO, K. K. K.; KUWAHARA, N.; FUJISHIGE, S.; ANDO, I., Characterization of poly (N-isopropylmethacrylamide) in water. *Polymer journal* **1990,** *22* (12), 1051-1057.
40. Pallecchi, E.; Chen, Z.; Fernandes, G.; Wan, Y.; Kim, J.; Xu, J., A thermal diode and novel implementation in a phase-change material. *Materials Horizons* **2015,** *2* (1), 125-129.
41. Zhao, D.; Qian, X.; Gu, X.; Jajja, S. A.; Yang, R., Measurement techniques for thermal conductivity and interfacial thermal conductance of bulk and thin film materials. *Journal of Electronic Packaging* **2016,** *138* (4), 040802.
42. Assael, M. J.; Dix, M.; Gialou, K.; Vozar, L.; Wakeham, W. A., Application of the Transient Hot-Wire Technique to the Measurement of the Thermal Conductivity of Solids. *International Journal of Thermophysics* **2002,** *23* (3), 615-633.
43. Dames, C., Measuring the thermal conductivity of thin films: 3 omega and related electrothermal methods. *Annual Review of Heat Transfer* **2013,** *16* (16).
44. Cahill, D. G.; Katiyar, M.; Abelson, J., Thermal conductivity of a-Si: H thin films. *Physical review B* **1994,** *50* (9), 6077.
45. Tong, T.; Majumdar, A., Reexamining the 3-omega technique for thin film thermal characterization. *Review of Scientific Instruments* **2006,** *77* (10), 104902.
46. Liu, W.; Balandin, A. A., Temperature dependence of thermal conductivity of Al x Ga 1− x N thin films measured by the differential 3 ω technique. *Applied physics letters* **2004,** *85* (22), 5230-5232.
47. Borca-Tasciuc, T.; Liu, W.; Liu, J.; Zeng, T.; Song, D. W.; Moore, C. D.; Chen, G.; Wang, K. L.; Goorsky, M. S.; Radetic, T., Thermal conductivity of symmetrically strained Si/Ge superlattices. *Superlattices and microstructures* **2000,** *28* (3), 199-206.
48. Koh, Y. K.; Singer, S. L.; Kim, W.; Zide, J. M.; Lu, H.; Cahill, D. G.; Majumdar, A.; Gossard, A. C., Comparison of the 3 ω method and time-domain thermoreflectance for measurements of the cross-plane thermal conductivity of epitaxial semiconductors. *Journal of Applied Physics* **2009,** *105* (5), 054303.

49. Huxtable, S. T., Time-Domain Thermoreflectance Measurements for Thermal Property Characterization of Nanostructures. *Handbook of Instrumentation and Techniques for Semiconductor Nanostructure Characterization (In 2 Volumes). Edited by Haight Richard A et al. Published by World Scientific Publishing Co. Pte. Ltd., 2012. ISBN# 9789814322843, pp. 587-610* **2012**, 587-610.
50. Jiang, P.; Huang, B.; Koh, Y. K., Accurate measurements of cross-plane thermal conductivity of thin films by dual-frequency time-domain thermoreflectance (TDTR). *Review of Scientific Instruments* **2016,** *87* (7), 075101.
51. Schmidt, A. J.; Chen, X.; Chen, G., Pulse accumulation, radial heat conduction, and anisotropic thermal conductivity in pump-probe transient thermoreflectance. *Review of Scientific Instruments* **2008,** *79* (11), 114902.
52. Rawat, V.; Koh, Y. K.; Cahill, D. G.; Sands, T. D., Thermal conductivity of (Zr, W) N/ScN metal/semiconductor multilayers and superlattices. *Journal of Applied Physics* **2009,** *105* (2), 024909.
53. Hopkins, P. E.; Reinke, C. M.; Su, M. F.; Olsson III, R. H.; Shaner, E. A.; Leseman, Z. C.; Serrano, J. R.; Phinney, L. M.; El-Kady, I., Reduction in the thermal conductivity of single crystalline silicon by phononic crystal patterning. *Nano letters* **2010,** *11* (1), 107-112.
54. Johnson, J. A.; Maznev, A. A.; Bulsara, M. T.; Fitzgerald, E. A.; Harman, T.; Calawa, S.; Vineis, C.; Turner, G.; Nelson, K. A., Phase-controlled, heterodyne laser-induced transient grating measurements of thermal transport properties in opaque material. *Journal of Applied Physics* **2012,** *111* (2), 023503.
55. Johnson, J. A.; Maznev, A.; Cuffe, J.; Eliason, J. K.; Minnich, A. J.; Kehoe, T.; Torres, C. M. S.; Chen, G.; Nelson, K. A., Direct measurement of room-temperature nondiffusive thermal transport over micron distances in a silicon membrane. *Physical review letters* **2013,** *110* (2), 025901.
56. Short, M. P.; Dennett, C. A.; Ferry, S. E.; Yang, Y.; Mishra, V. K.; Eliason, J. K.; Vega-Flick, A.; Maznev, A. A.; Nelson, K. A., Applications of transient grating spectroscopy to radiation materials science. *JOM* **2015,** *67* (8), 1840-1848.
57. Cuffe, J.; Eliason, J. K.; Maznev, A. A.; Collins, K. C.; Johnson, J. A.; Shchepetov, A.; Prunnila, M.; Ahopelto, J.; Torres, C. M. S.; Chen, G., Reconstructing phonon mean-free-path contributions to thermal conductivity using nanoscale membranes. *Physical Review B* **2015,** *91* (24), 245423.
58. Minnich, A. J., Multidimensional quasiballistic thermal transport in transient grating spectroscopy. *Physical Review B* **2015,** *92* (8), 085203.
59. Kim, T.; Ding, D.; Yim, J.-H.; Jho, Y.-D.; Minnich, A. J., Elastic and thermal properties of free-standing molybdenum disulfide membranes measured using ultrafast transient grating spectroscopy. *APL Materials* **2017,** *5* (8), 086105.
60. Goodno, G. D.; Dadusc, G.; Miller, R. D., Ultrafast heterodyne-detected transient-grating spectroscopy using diffractive optics. *JOSA B* **1998,** *15* (6), 1791-1794.
61. van der Tempel, L.; Melis, G. P.; Brandsma, T., Thermal conductivity of a glass: I. Measurement by the glass–metal contact. *Glass physics and chemistry* **2000,** *26* (6), 606-611.
62. Ramires, M. L.; Nieto de Castro, C. A.; Nagasaka, Y.; Nagashima, A.; Assael, M. J.; Wakeham, W. A., Standard reference data for the thermal conductivity of water. *Journal of Physical and Chemical Reference Data* **1995,** *24* (3), 1377-1381.
63. Schmidt, A. J. Optical characterization of thermal transport from the nanoscale to the macroscale. Massachusetts Institute of Technology, 2008.
64. Haar, L.; Gallagher, J.; Kell, G., NBS/NRC Steam Tables Hemisphere Publishing Corporation Washingdon. *DC Google Scholar* **1984**.
65. Marsh, K. N.; Marsh, K., *Recommended reference materials for the realization of physicochemical properties*. Blackwell Scientific Publications Oxford, UK: 1987.
66. Sengers, J.; Watson, J. T. R., Improved international formulations for the viscosity and thermal conductivity of water substance. *Journal of physical and chemical reference data* **1986,** *15* (4), 1291-1314.
67. Archer, D. G.; Wang, P., The Dielectric Constant of Water and Debye‐Hückel Limiting Law Slopes. *Journal of physical and chemical reference data* **1990,** *19* (2), 371-411.
68. Vargaftik, N.; Volkov, B.; Voljak, L., International tables of the surface tension of water. *Journal of Physical and Chemical Reference Data* **1983,** *12* (3), 817-820.
69. Xie, X.; Li, D.; Tsai, T.-H.; Liu, J.; Braun, P. V.; Cahill, D. G., Thermal Conductivity, Heat Capacity, and Elastic Constants of Water-Soluble Polymers and Polymer Blends. *Macromolecules* **2016,** *49* (3), 972-978.
70. Foster, K. R.; Cheever, E.; Leonard, J. B.; Blum, F. D., Transport properties of polymer solutions. A comparative approach. *Biophysical journal* **1984,** *45* (5), 975-984.

71. Lu, Y.; Ye, X.; Li, J.; Li, C.; Liu, S., Kinetics of laser-heating-induced phase transition of poly (N-isopropylacrylamide) chains in dilute and semidilute solutions. *The Journal of Physical Chemistry B* **2011,** *115* (42), 12001-12006.
72. Yin, X.; Hoffman, A. S.; Stayton, P. S., Poly (N-isopropylacrylamide-co-propylacrylic acid) copolymers that respond sharply to temperature and pH. *Biomacromolecules* **2006,** *7* (5), 1381-1385.
73. Lin, S.-Y.; Chen, K.-S.; Liang, R.-C., Thermal micro ATR/FT-IR spectroscopic system for quantitative study of the molecular structure of poly (N-isopropylacrylamide) in water. *Polymer* **1999,** *40* (10), 2619-2624.
74. Katsumoto, Y.; Tanaka, T.; Sato, H.; Ozaki, Y., Conformational Change of Poly (N-isopropylacrylamide) during the Coil− Globule Transition Investigated by Attenuated Total Reflection/Infrared Spectroscopy and Density Functional Theory Calculation. *The Journal of Physical Chemistry A* **2002,** *106* (14), 3429-3435.
75. Tian, Z.; Marconnet, A.; Chen, G., Enhancing solid-liquid interface thermal transport using self-assembled monolayers. *Applied Physics Letters* **2015,** *106* (21), 211602.
76. Ge, Z.; Cahill, D. G.; Braun, P. V., Thermal conductance of hydrophilic and hydrophobic interfaces. *Physical review letters* **2006,** *96* (18), 186101.
77. Harikrishna, H.; Ducker, W. A.; Huxtable, S. T., The influence of interface bonding on thermal transport through solid–liquid interfaces. *Applied Physics Letters* **2013,** *102* (25), 251606.
78. Tian, Z.; Hu, H.; Sun, Y., A molecular dynamics study of effective thermal conductivity in nanocomposites. *International Journal of heat and mass transfer* **2013,** *61*, 577-582.